H–D Isotope and Chain-Length Dependence of Phase Separation in Quenched *n*-Alkane Binary Combinations in the Crystalline State

Douglas L. Dorset*

Electron Diffraction Department, Hauptman–Woodward Medical Research Institute, Inc., 73 High Street, Buffalo, New York 14203-1196

Robert G. Snyder

Department of Chemistry, University of California, Berkeley, California 94720-1460

Received June 15, 1995; Revised Manuscript Received September 18, 1995[⊗]

ABSTRACT: Certain binary *n*-alkane combinations, quenched to room temperature from the comelt, form metastable solid solution crystals that subsequently undergo spontaneous demixing. The degree and rate of phase separation are known to depend upon the chain-length difference of the two components. Recently, we have found that, in addition to the chain-length difference, the isotopic composition (H or D) can also be an important factor affecting the separation. We report here electron diffraction and calorimetric measurements, revealing the relative tendencies for microphase separation for the four possible isotopic combinations in C_{30}/C_{36} (depending on whether each ingredient is perhydrogenated or perdeuterated). The isotope effect on phase stability is shown to be qualitatively similar to that of changing the chain-length difference, if the volume difference between CH_2 and CD_2 methylene groups, respectively, is expressed in terms of chain length. This trend is explored further for binaries $C_{30}/C_{n'}$, where n' is systematically increased. Measurements made in this study are then compared to those from vibrational spectroscopy.

Introduction

Deuterium substitution for hydrogen often is employed to form a tagged molecule or molecular moiety as a probe for structural studies. It is usually assumed that this substitution is nonperturbing, and, indeed, this is generally the case, especially if the isotopic replacement is localized to a relatively small region of the molecule. For example, in NMR[1] and infrared[2] spectroscopic measurements, a CD_2 group is inserted at a specific site in a polymethylene chain to determine local conformation and dynamic behavior.

On the other hand, replacing all of the hydrogen atoms in a molecule with deuterium can significantly modify the phase behavior of the system if hydrogen is a major molecular component, as is the case for hydrocarbon chains. It is known, for example, that binary combinations of the perhydrogenated and perdeuterated forms of high molecular weight polymers may undergo some degree of chain separation.[3] Buckingham and Hentschel[4] offered an explanation for this phenomenon in terms of a reduced mixing entropy that occurs when going from low to high molecular weight chains. A corollary of their explanation is that the separation of low molecular weight combinations, *n*-alkanes, for example, will be negligible when the chains are of nearly equal length.

By contrast, we have recently reported conditions whereby isotopic substitution can significantly, sometimes spectacularly, affect the miscibility of components in crystalline binary combinations consisting of short chains.[5–7] This phenomenon, observed for alkane binaries with chains less than 40 carbons, is fundamentally different from that for high polymers. It is most pronounced when the quenched solid consisting of perhydrogenated components is metastable. For such a binary, the extent and rate of demixing can be highly influenced by the isotopic composition.

[⊗] Abstract published in *Advance ACS Abstracts,* November 1, 1995.

Few studies have been reported in which the phase behavior of perhydrogenated and perdeuterated polymethylene chains has been compared in a systematic way. Recently, we have found[8] that the melting point difference between the two *n*-alkane isotopes—known previously to be of the order of 3–4 K for long chains—is dependent on chain length. This difference was found to be approximately proportional to the average of the melting points for each isotopic pair, a relation derivable from the principle of corresponding states.[8]

Electron diffraction has been used[9] to compare the crystal structures of the H and D chain analogs of *n*-paraffins. The results generally confirmed, within the accuracy of the measurements (typically about 5% for unit cell constants), the accepted view that the structures are essentially the same. For example, measured unit cell parameters, and even quantitative analyses of layer packing, based on electron diffraction data reveal no discernible differences. Small differences, however, were found just below the melting point. This study also included a determination of the phase diagrams for binary combinations of H and D chain isotopes for the same *n*-alkane. The temperature of the DSC endotherm peak observed for the "premelting" and melting transitions at various molar concentrations were near those computed when assuming ideal cosolubility. From these measurements, then, it would be assumed that the influence of a perdeuterated molecule as a structural probe in such binaries would be nonperturbative. However, as we shall demonstrate here, exceptions may occur for metastable solid solutions.

This paper extends the earlier electron diffraction and calorimetric evaluation of equal-length hydrocarbon/deuterocarbon binaries[9] to combinations where the chain lengths differ. Specifically, the binary C_{30}/C_{36}, which had been shown to form metastable solid solutions for perhydrogenated components when quenched from the melt, is the major object of this study, using the addition of perdeuterated component as the major variable. The connection between the isotope and chain-

0024-9297/95/2228-8412$09.00/0

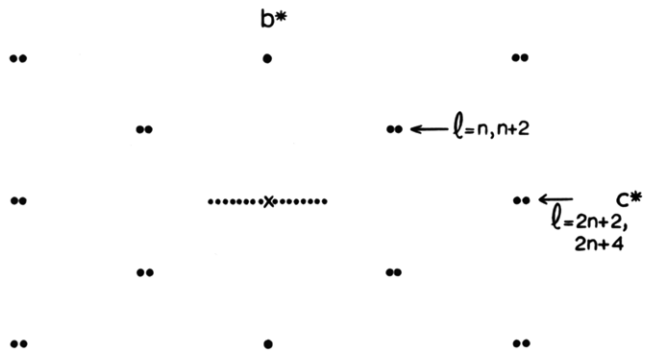

Figure 1. Schematic depiction of a 0kl electron diffraction pattern from an orthorhombic n-paraffin. For pure samples or their solid solutions, comparison of the 00l spacing to the spacing along c^* for the most intense 01l pair can be used to determine the average chain length of a lamella. Hence $l = n, n + 2$, corresponds to the average chain length n-C_nH_{2n+2}.

length effects is discussed after extended studies with n-$C_{30}D_{62}$/n-$C_{n'}H_{2n'+2}$, where $n' \geq 30$. Also included are vibrational spectroscopic determinations of domain size and conformational disorder for these and related binaries. We discuss the problem of correlating, in a meaningful way, diffraction and spectroscopic results.

Experimental Procedures

A. Samples and Calorimetry. Sources and physical properties of the hydrogenated and deuterated n-alkanes used in this study have been detailed in earlier publications.[8-10] Binary solids of varying concentration were prepared by quenching the comelt to room temperature.

A Mettler TA3300 differential scanning calorimeter was used to measure the thermal properties of the binary solids. Samples were weighed into aluminum pans which were then sealed. After fusing the solids by quenching from the melt, the samples were measured at various times after the quench. The temperature scale for these scans was calibrated against the known melting points of a series of n-paraffins.[8] (When needed, the enthalpy of a phase transition was calibrated against the known value for indium metal.) Phase diagrams were then constructed from the DSC curves, the boundaries between phases being defined, in this study, as the peak temperatures of the endotherms.

After the DSC measurements were made, the samples were removed from the opened aluminum pans. A small amount of solid was then dissolved in petroleum ether, and the remaining paraffin film, formed when the solution was evaporated, was recrystallized from a comelt from benzoic acid diluent to form an epitaxially oriented paraffin sample.[11,12] After removal of the benzoic acid by sublimation in vacuum, the paraffin samples were suitable for electron diffraction measurements.

B. Electron Diffraction Measurements. Selected-area electron diffraction experiments were carried out at 100 kV with a JEOL JEM-100CXII electron microscope.[13] Usual precautions were taken to minimize the radiation exposure to the organic microcrystals. The diffraction pattern camera length was calibrated with known spacings for the powder pattern of gold (deposited on the grid surface by evaporation in a vacuum chamber). In some experiments, the samples were heated in a GATAN 626 stage to permit observation at elevated temperatures.

Characteristics of the 0kl electron diffraction patterns from n-paraffins and their binaries, in either of two orthorhombic structures (space group $Pca2_1$ or $A2_1am$), have been discussed at length in earlier papers.[10,14] Aside from their definite utility for quantitative structure determinations, the indexing of major reflections (Figure 1) can be used qualitatively to describe the average layer structure of any microcrystalline area. When first quenched from the melt, the binary solids behave in this respect as if they are stable solid solutions. Comparison of the lamellar spacing d_{00l} with the spacing of

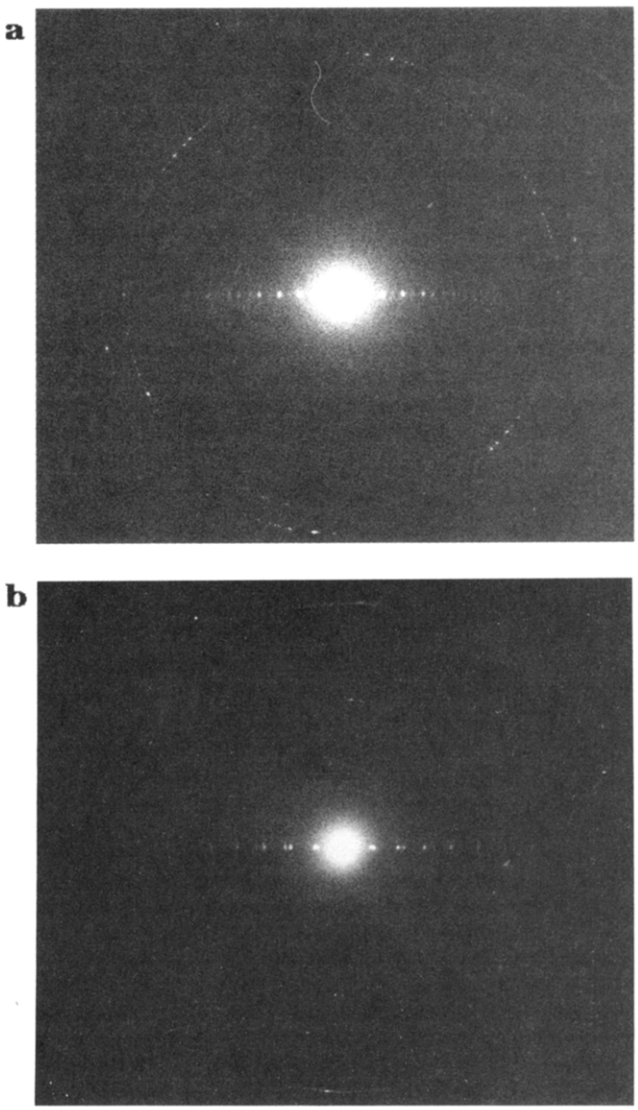

Figure 2. The type of "superlattice" array that appears on the 00l row of a 01l electron diffraction pattern when e.g. C_{30}/C_{36} binaries undergo demixing: (a) when the isotopic combinations are H/H, H/D, or D/D; (b) when the isotopic combination is D/H.

the two most intense 01l reflections along the c^* direction permits this determination to be made because $l = n, n + 2$, where n is the average chain length (expressed as the number of carbons) of the lamella in the microcrystalline region. The average chain length, converted to a lamellar thickness, agrees well with the measured lamellar spacing, based on the compilation made by Nyburg and Potworowski[15] for pure orthorhombic n-paraffins. Moreover, for any nominal bulk concentration, it can be shown that several, different, crystal structures can exist in contiguous microcrystalline regions, mimicking an average even- or odd-chain paraffin. As the solid ages, an apparent superlattice can form (Figure 2) wherein the lamellar 00l row no longer corresponds to one single spacing. (The most intense reflections at low angle still may correspond to the original solid solution spacing.) The solid is more ordered than before because the resolution of the lamellar row increases with time. There are reasons to expect that there is an incommensurate phase growing from the metastable solid solution, and a representative lamellar sequence has been suggested in an earlier study.[16]

Results

First, it will be useful to define, as clearly as possible, the terms used to describe the various states expressed by the binary solids. A "stable" combination is defined

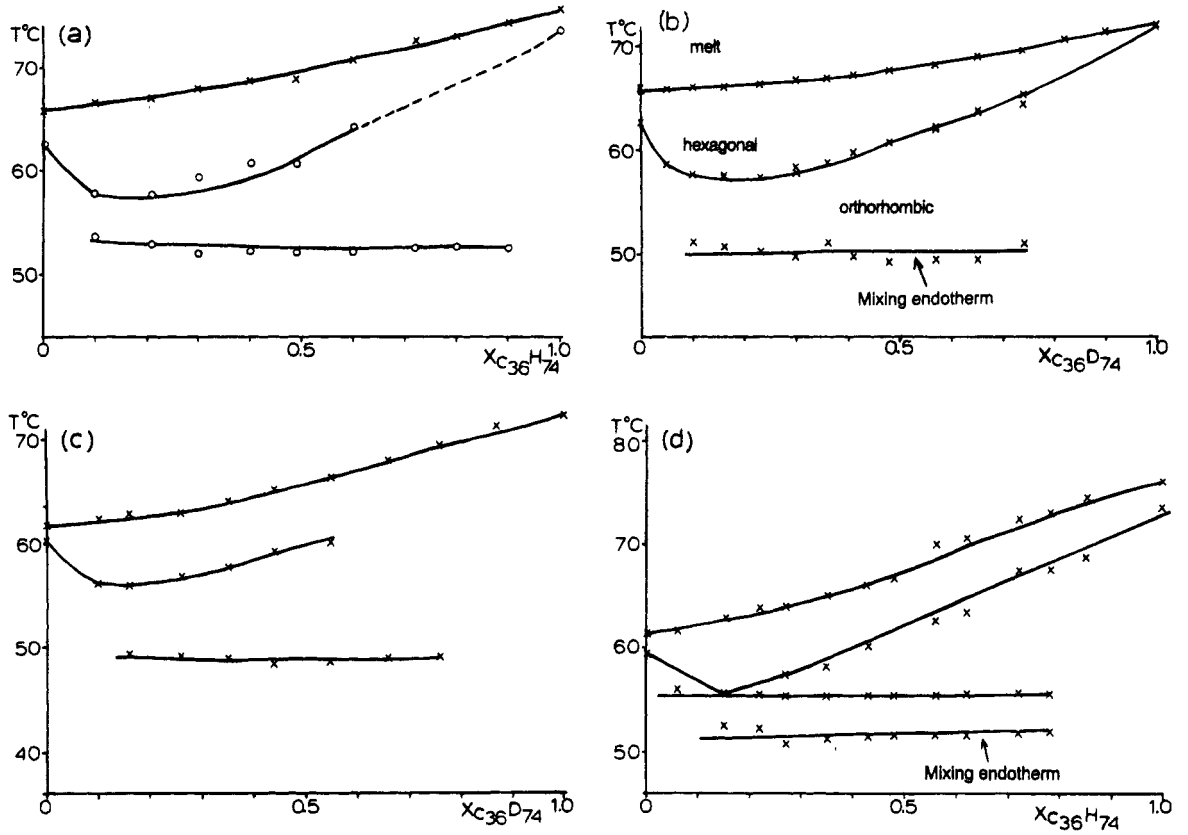

Figure 3. Phase diagrams for C_{30}/C_{36} combinations: (a) n-$C_{30}H_{62}/n$-$C_{36}H_{74}$; (b) n-$C_{30}H_{62}/n$-$C_{36}D_{74}$; (c) n-$C_{30}D_{62}/n$-$C_{36}D_{74}$; (d) n-$C_{30}D_{62}/n$-$C_{36}H_{74}$. Note that the mixing endotherms, observed as apparent isotherms over concentration, do not correspond to the theoretical intersection of liquidus curves when a theoretical phase diagram is computed (see ref 10).

here as a solid solution that remains randomly comixed for an indefinitely long time. There are also two types of "unstable" solid, defined by the occurrence of demixing during or just after the quench from the melt to room temperature or at a later time. Thus a "metastable" solid appears to be a stable solid solution just after quenching but later undergoes spontaneous demixing. A "fractionated" solid is one that is more or less demixed immediately during or just after the quench to ambience. Criteria used to make these classifications are based on the results of electron diffraction and DSC measurements.

A. Isotopic Combinations for C_{30}/C_{36}. These binary solids, with a common average chain length and chain length difference, have four isotopic variants, designated at $C_{30}{}^{i}/C_{36}{}^{i'}$, where i or i′ = H or D. The solid for which i = i′ = H lies near a boundary, which is based on chain-length differences, that separates stable from unstable binaries.[10] It is for this reason that the phase behavior of the C_{30}/C_{36} combination is highly sensitive to hydrogen/deuterium substitution. This sensitivity to isotopic composition is reflected by changes in the degree and rate of their demixing upon quenching.

1. $C_{30}H_{62}/C_{36}H_{74}$ Binary. The all-hydrogenated ($C_{30}{}^{H}/C_{36}{}^{H}$) combination has been the subject of earlier calorimetric and electron diffraction studies. Its phase diagram (Figure 3a), if derived from DSC curves for samples freshly crystallized from the melt, is typical for n-alkane solid solutions. However, if the DSC curves are measured after the samples have aged at room temperature for a few days, a new endotherm appears. This new endotherm indicates that the binary solid solution is metastable. It is associated with the dissolution of domains of phase-separated components. For this reason, we have referred to it as the "mixing" endotherm.[17] It appears in the DSC scans of aged binary solids over a wide range of concentrations, specifically mole fractions of n-$C_{36}H_{74}$ from ca. 0.1 to 0.9.

A somewhat more direct indication of microphase separation is found in the electron diffraction patterns from aged binaries, which show the 00l reflections to transform to a "superlattice-like" motif,[10,16] apparently associated with the random sequence of lamellae in localized microstructures. If the temperature of this solid (in the electron microscope) is increased beyond the temperature of the "mixing" endotherm described above, the solid solution sequence, i.e., one lamellar spacing, is observed in the electron diffraction pattern. Hence, the endotherm is confirmed to represent a dissolution of any microdomains formed in the aged binary solids, as identified by this diffraction probe.

Superlattice-like microcrystalline structures of the kind described earlier are present in aged solids over a wide range of concentrations. A plot of the average lamellar spacing for the most intense low-angle sequence of reflections (corresponding to a single repeat) vs concentration falls just slightly above the straight line connecting the spacings of the pure components (Figure 4a). Thus, Vegard's criterion for a solid solution is met, even though the solid is heterogeneous at the microcrystalline level. Likewise, the equivalent average chain lengths for the lamellar repeat, obtained from the 01l reflections as described above, parallels the behavior found for stable solid solutions, since several contiguous crystal structures are observed at any nominal bulk concentration of components (Figure 5a).

2. $C_{30}H_{62}/C_{36}D_{74}$ and $C_{30}D_{62}/C_{36}D_{74}$ Solids. The H/D ($C_{30}{}^{H}/C_{36}{}^{D}$) and D/D ($C_{30}{}^{D}/C_{36}{}^{D}$) combinations are also metastable. Their DSC scans, phase diagrams

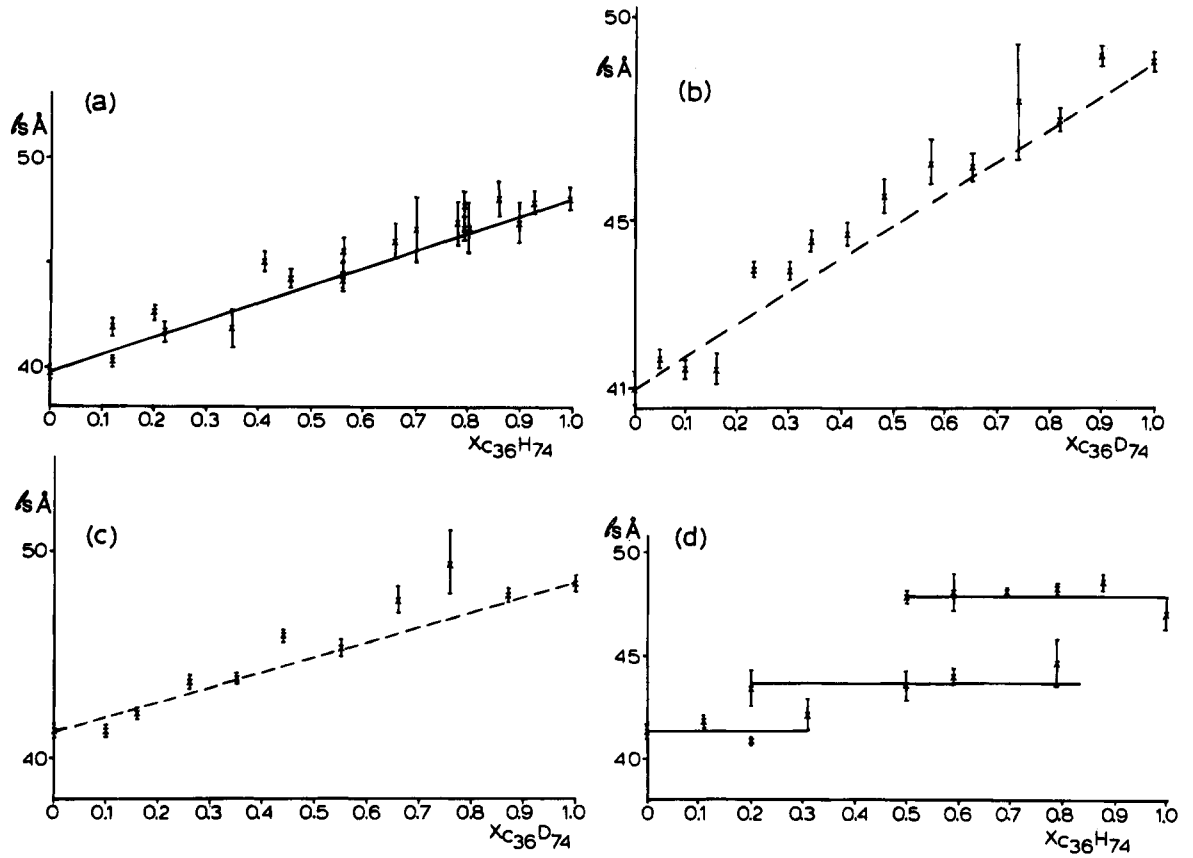

Figure 4. Plots of average lamellar spacings with increasing concentration of C_{36} in C_{30}/C_{36} binaries: (a) n-$C_{30}H_{62}/n$-$C_{36}H_{74}$; (b) n-$C_{30}H_{62}/n$-$C_{36}D_{74}$; (c) n-$C_{30}D_{62}/n$-$C_{36}D_{74}$; (d) n-$C_{30}D_{62}/n$-$C_{36}H_{74}$.

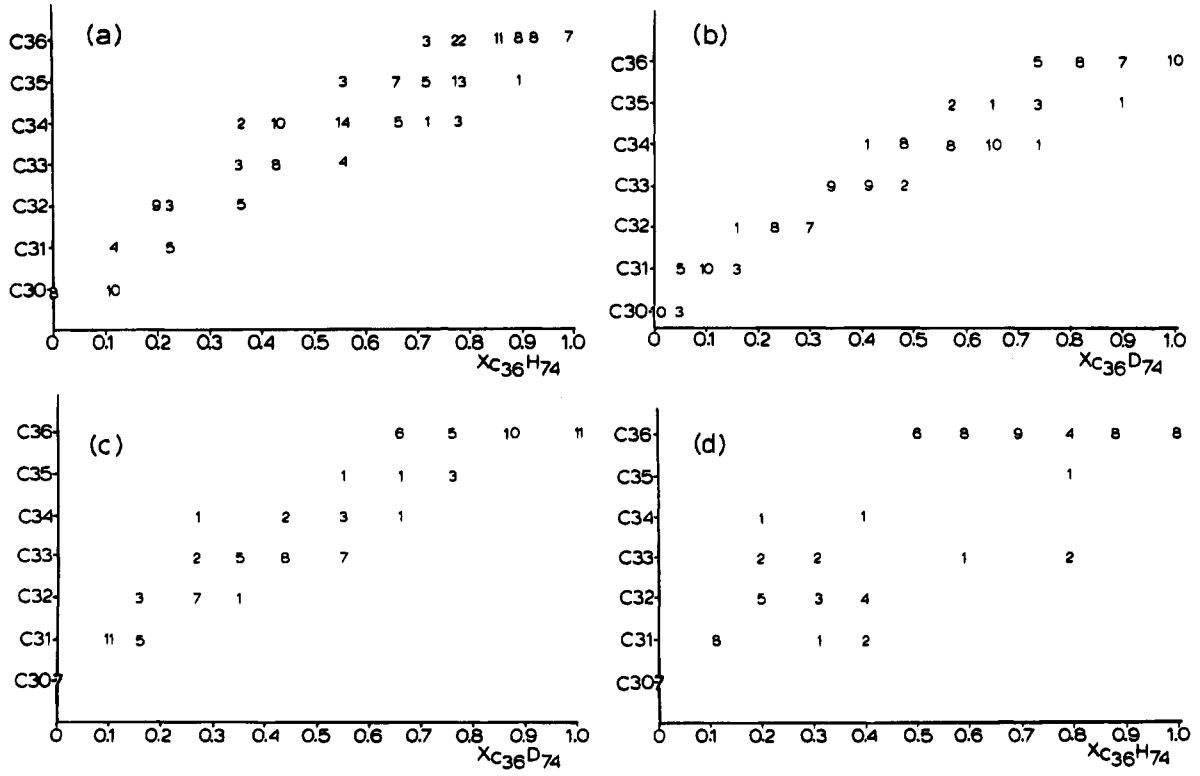

Figure 5. Local crystal structures of C_{30}/C_{36} binaries for nominal concentrations of C_{36}. The figures indicate numbers of microcrystals in a sample that correspond to the indicated chain structure at concentration $X_{C_{36}}$: (a) n-$C_{30}H_{62}/n$-$C_{36}H_{74}$; (b) n-$C_{30}H_{62}/n$-$C_{36}D_{74}$; (c) n-$C_{30}D_{62}/n$-$C_{36}D_{74}$; (d) n-$C_{30}D_{62}/n$-$C_{36}H_{74}$.

(Figure 3b,c), and electron diffraction patterns are similar to those observed for $C_{30}{}^{H}/C_{36}{}^{H}$. Electron diffraction patterns from the aged solids have typical superlattice-like lamellar reflections. From the indices of the patterns, local crystal structures are found, as before, again similar to $C_{30}{}^{H}/C_{36}{}^{H}$. When the samples are heated to a temperature above that of the mixing endotherm, the lamellar row again resembles that of a

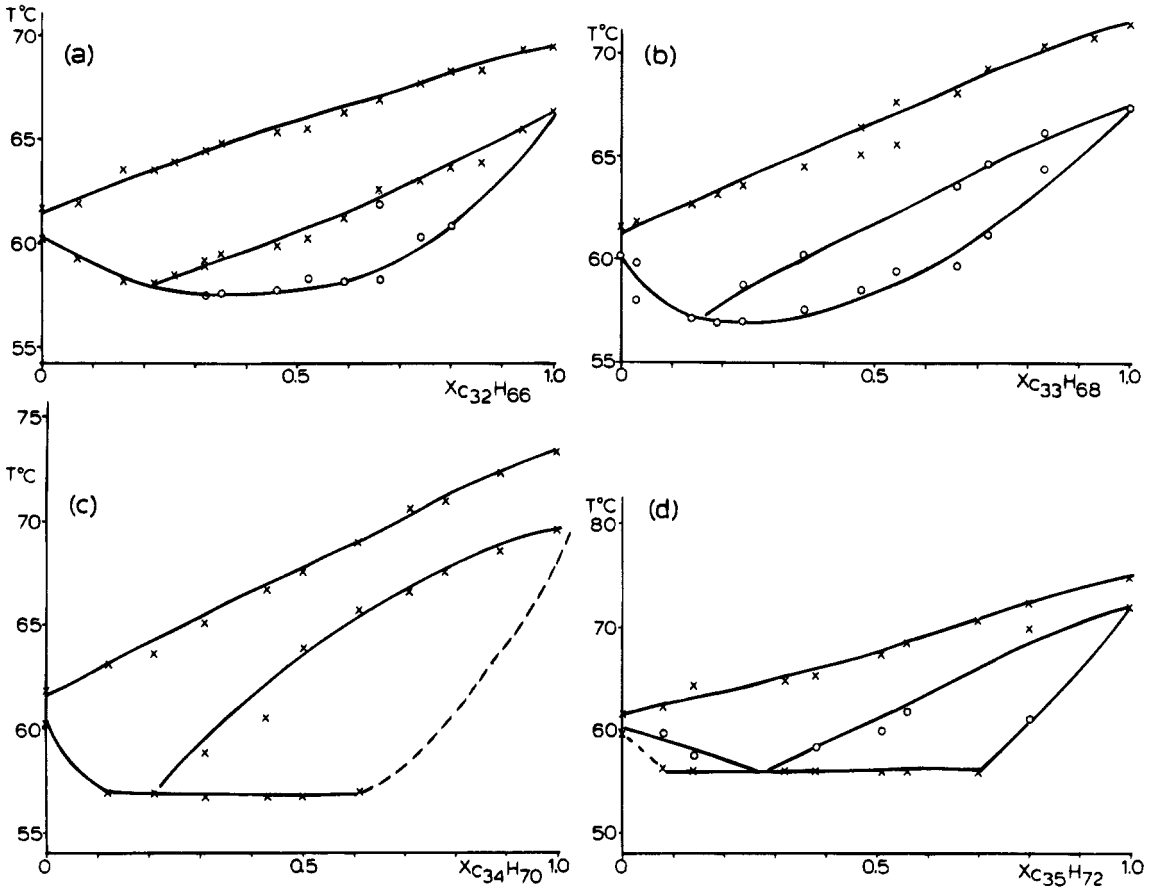

Figure 6. Phase diagrams of n-$C_{30}D_{62}$ with n-$C_{n'}H_{2n'+2}$: (a) $n' = 32$; (b) $n' = 33$; (c) $n' = 34$; (d) $n' = 35$. In all cases, a nearly ideal solid solution exists in the "rotator" phase.

stable solid solution, and average lamellar spacings lie slightly above the line determined from Vegard's law (Figure 4b,c). Similar to the above case, there are distributions of local crystal structures for any molar concentration (Figure 5b,c).

3. $C_{30}D_{62}/C_{36}H_{74}$ Solid. The D/H (C_{30}^{D}/C_{36}^{H}) combination, freshly quenched to room temperature, is a fractionated solid. In the temperature region just below the melting point, the phase diagram (Figure 3d) is similar to the other isotopic combinations of C_{30}/C_{36}, because the components form solid solutions. The DSC curves of aged mixtures also contain the mixing endotherm.

At lower temperatures, however, the phase behavior of C_{30}^{D}/C_{36}^{H} departs significantly from that of the other isotopic combinations. The phase diagram resembles the one found for a eutectic of solid solutions[10,16], e.g., n-$C_{30}H_{62}/n$-$C_{40}H_{82}$. In the plot of average lamellar spacing vs concentration, this fractionation is revealed by the occurrence of constant spacings over wide concentration ranges (Figure 4d). Average structures obtained from the 01l indices also indicate constant lamellar structure for these regions (Figure 5d). The solids associated with these data have been interpreted in terms of a crystal structure where domains of different average structures are closely associated across a methyl end-plane surface.[16]

B. Binary Compositions with $C_{30}D_{62}$ as a Common Component. Electron diffraction measurements were made on a homologous series of binary solids n-$C_{30}D_{62}/n$-$C_{n'}H_{2n'+2}$, i.e., in which all have the C_{30}^{D} component is a common shorter member. It is of interest to determine the value of n' (=30, 32, 33, 34, or 35) at which phase separation first appears.

Figure 6 depicts the phase diagrams of these binaries, omitting C_{30}^{D}/C_{30}^{H}, the one for the equal chain length combination that had been published earlier[9] and shown to be nearly ideal. In the series C_{30}^{D}/C_{32}^{H}, C_{30}^{D}/C_{33}^{H}, C_{30}^{D}/C_{34}^{H}, C_{30}^{D}/C_{35}^{H}, all solids give diffraction patterns characteristic of stable solid solutions when examined near the time of their growth from the melt. This behavior is manifested by both the appearance of the phase diagrams and the appearance of a single 00l lamellar row of reflections in the 0kl electron diffraction patterns. However, if C_{30}^{D}/C_{35}^{H} is allowed to age for a year, a superlattice-like array of 00l reflections appears in the electron diffraction pattern, associated with the appearance of the mixing endotherm mentioned above. The slow demixing of C_{30}^{D}/C_{35}^{H}, therefore, resembles that found by Mazee[18] from X-ray measurements on C_{30}^{H}/C_{35}^{H} for a sample aged for a comparable time. (His observation has been verified in electron diffraction studies.[10])

Discussion

On the basis of DSC and electron diffraction measurements, we found that three of the four possible isotopic combinations of freshly melt-quenched C_{30}/C_{36} (i.e., H/H, D/D, and H/D) form metastable solid solutions that slowly demix. The D/H combination is quite different since it is highly fractionated just after the quench. These results invite comparison to and correlation with the results of earlier studies.

Infrared spectroscopy can measure quantitatively the degree of demixing and lateral domain size and the time dependence of these quantities; Raman spectroscopy can measure conformational disorder in the chains. Thus,

spectroscopy and diffraction provide complementary information about the phase separation mechanism. On the other hand, results from these two probes may sometimes be difficult to reconcile because they measure different kinds of structural parameters. In this particular study, the difference is expressed by structural changes in the longitudinal direction by diffraction experiments and in the lateral direction by infrared experiments.

A specific illustration of the different structural changes can be given. Using infrared methods, it is possible to measure and monitor domains with lateral dimensions no larger than several alkane chains. Domains this small are essentially undetectable in Bragg diffraction experiments (and would only be visualized as a weak, possibly directional, diffuse component). For a metastable mixture, such as C_{30}^{H}/C_{36}^{D}, spontaneous demixing begins shortly after the quench, and the lateral growth of the domains can be monitored henceforth by spectroscopic means.[17] Changes in the lamellar electron diffraction intensities appear relatively much later, however, perhaps a few days after the quench, at a time when the domains have become large enough to allow a critically well-defined longitudinal periodicity to be expressed by Bragg diffraction. The reflections may appear somewhat suddenly, giving the impression of a discontinuous structural change, which is not reflected in the generally smooth domain growth curves determined from infrared spectroscopic measurements.

A. H/D and D/H Binaries. Recently reported infrared measurements[7,17] indicate that freshly recrystallized H/D and D/H binaries differ significantly in their degree of demixing just after the quench. Although these differences do not appear to be as large as those observed in the electron diffraction measurements, possibly for the reasons discussed above, both techniques clearly indicate that the immediate phase separation for D/H is much greater than that of H/D, so that the binaries are, respectively, fractionated and metastable solids. The infrared measurements also indicate that both binaries undergo spontaneous microphase separation, with the rate being largest for the D/H combination.

B. H/H and D/D Combinations. Given the large difference between H/D and D/H, is it also possible to distinguish phase separation behavior for H/H, D/D, and H/D solids, which have, so far, been grouped together under a common phenomenological description? Actually, there is good reason to expect significant differences. For example, while the stabilities of the H/H and D/D binaries are nearly identical, they are intermediate between H/D and D/H. One basis for distinction is the increased tendency for any combination to demix as the difference of melting points for the ingredients increases. For the C_{30}/C_{36} combinations, the melting point differences for D/H, H/H, D/D, and H/D are, respectively, 14.6, 10.5, 10.5, and 6.4 K. (In using the melting points of the components, a constant value of 4.1 K was assumed for the melting point difference between the hydrogenated and perdeuterated form of any given n-alkane.[8]) Thus, the predicted tendency to demix is D/H > H/H = D/D > H/D.

Calorimetric and diffraction measurements tend to support this order. (The infrared technique cannot be applied here to H/H and D/D binaries since the isotopes must be different to obtain a measurement.) The position of D/H in this series is clearly correct. To help place the other combinations, we have used the relative

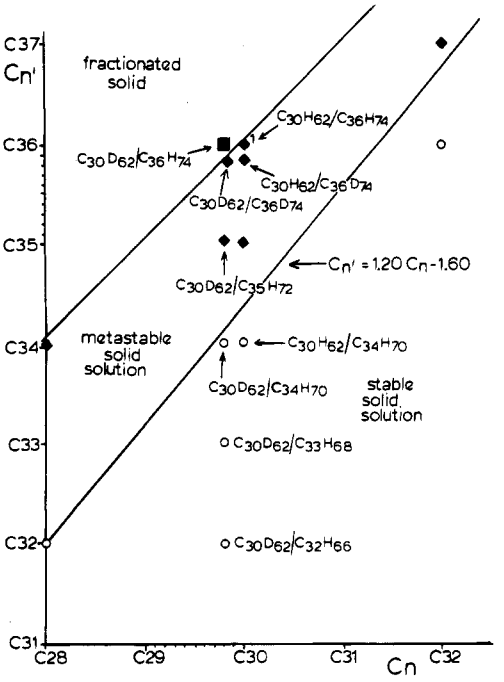

Figure 7. Plots of C_n vs $C_{n'}$ indicating binary phase behavior and defining three domains. The line at the right, defining the boundary between stable and metastable solid solutions, is drawn at $C_{n'} = 1.20C_n - 1.60$. The line separating metastable solid solutions from fractionated solids is drawn to divide the phases observed for C_{30}/C_{36} binaries at different isotopic combinations (see text). Here points representing stable solid solutions, metastable solid solutions, and fractionated solids are given the respective legends (○), (◆), and (■).

value of the enthalpy associated with the "mixing" endotherm, since this endotherm is due to the thermally induced dissolution of microdomains.[21] The enthalpy of the mixing endotherm is found to be smallest for the H/D combination when all isotopic mixtures have been aged for comparable times. Electron diffraction measurements provide additional information here. In the characterization of local crystal structures (Figure 5), the distribution is found to be narrowest for H/D, which is interpreted to indicate greater compositional homogeneity (i.e., greater randomness).

The various isotopic combinations can be fitted to a "phase map" (Figure 7), of a type discussed before.[10,19] Such a map has coordinates n and n' that correspond, respectively, to short and long chain lengths of a binary solid. If various binary mixtures ($C_n^{H}/C_{n'}^{H}$) are positioned on it, those with similar stabilities group together. Straight-line boundaries can be drawn that separate solid solutions, metastable solid solutions, and fractionated solids. In Figure 7, a region of this map is shown where $n = 28-32$ and $n' = 31-37$.

The isotopic combinations of C_{30}/C_{36} fall into their positions on Figure 7 if we adjust the lengths (n and n') of the component chains to account for the molar volume decrease of about 0.5% that occurs when CD_2 is substituted for CH_2. The adjustment for this binary combination is based on the volume change when C_{33} is perdeuterated, i.e., the alkane that has an average length of the components. This corresponds to a chain-length decrease of about 0.15 carbons or for the respective isotopic combinations: H/D (30.00, 35.85), D/D (29.85, 35.85), H/H (30.00, 36.00), D/H (29.85, 36.00). Thus, in addition to the previously determined sharp boundary between the stable and metastable solid solutions, there also appears to be an equally sharp

boundary between metastable solid solutions and fractionated binaries (Figure 7).

C. $C_{30}^{D}/C_{n'}^{H}$ and $C_{30}^{H}/C_{n'}^{H}$ Series. Electron diffraction and calorimetry indicate that freshly quenched binaries $C_{30}^{D}/C_{n'}^{H}$, where $n' = 30$, 32, 33, or 34, are stable solid solutions. Similar to the findings on all-hydrogenated[18] systems, however, the combination $n' = 35$ is found to be demixed after a year's standing.

Recent Raman determinations[22] of conformational disorder in binary n-alkane mixtures in this chain-length region provide complementary insight in understanding how the chain-length difference and the tendency of the components to separate are related. Raman spectra measure conformational disorder in the region of the chain nearest its end. Such measurements show that the dependence of the disorder on the chain-length difference is continuous, albeit rather complex. The concentration of gauche bonds reaches a maximum at a chain-length difference of around 5–6 carbons. If the difference becomes much less or much larger, the disorder decreases dramatically.

This behavior was found in the case of a series of freshly quenched mixtures, $C_{30}^{H}/C_{n'}^{H}$, where $n' = 30$–34, 36, 38, and 40. The molar ratio of the components was 1:1 and the mixtures were at room temperature. With increasing n' (or, equivalently, with increasing chain-length difference), the conformational disorder initially increased, beginning with $n' = 30$ (that is pure C_{30}^{H}) and up to $n' = 35$, at which point maximum disorder was reached. Increasing n' further resulted in decreasing disorder. For $n' = 40$, which mixture in this series has the largest chain-length difference, the disorder is quite low, comparable to that for the pure n-alkanes.

These observations are explicable in terms of the dependence of the stability of the mixtures on the chain-length mismatch. If the mismatch is relatively small, solid solution stability is attained by the filling of void space in the interfacial region via chain-end rearrangement. This necessarily involves gauche bonds, and therefore conformational disorder. One expected manifestation of the void filling would be smoother interlamellar surfaces. In fact, electron diffraction structure analysis[23] and lamellar surface probes[24] reveal that the chain end regions are still well-defined planes. (The samples examined were simple binary solid solutions, as well as a low molecular weight polyethylene fraction and two multicomponent paraffin waxes.)

As the chain-length mismatch increases, a point is reached at which greater stability can be attained through demixing than through interfacial chain-end rearrangements. Demixing leads to fractionation, in which the domains consist primarily of one component. Thus, more ordered packing becomes possible and, as a consequence, overall conformational disorder is reduced. The intermediate case, where the stability provided by on-site rearrangement of the chain ends is comparable to that resulting from phase separation, leads to the formation of metastable mixtures of the kind described in this paper.

Acknowledgment. The authors gratefully acknowledge support for this research by the National Science Foundation (originally Grant DMR86-10783 to the Medical Foundation of Buffalo, Inc.) and by the National Institute of General Medical Sciences (Grant GM 27690 to the University of California at Berkeley).

References and Notes

(1) Dybowski, C.; Brandolini, A. J. In *Characterization of Solid Polymers*; Spells, S. J., Ed.; Chapman & Hall: London, 1994; p 276ff.
(2) Maroncelli, M.; Strauss, H. L.; Snyder, R. G. *J. Phys. Chem.* **1985**, *89*, 5260.
(3) Bates, F. S.; Fetters, L. J.; Wignall, G. D. *Macromolecules* **1988**, *21*, 1086.
(4) Buckingham, A. D.; Hentschel, H. G. E. *J. Polym. Sci., Polym. Phys. Ed.* **1980**, *18*, 853.
(5) White, J. W.; Dorset, D. L.; Epperson, J. E.; Snyder, R. G. *Chem. Phys. Lett.* **1990**, *166*, 560.
(6) Snyder, R. G.; Kim, Y.; Strauss, H. G.; Goh, M. C. *Polym. Prepr. (Am. Chem. Soc., Div. Polym. Chem.)* **1989**, *30* (2), 295.
(7) Snyder, R. G.; Srivatsavoy, V. J. P.; Cates, D. A.; Strauss, H. L.; White, J. W.; Dorset, D. L. *J. Phys. Chem.* **1994**, *98*, 674.
(8) Dorset, D. L.; Strauss, H. L.; Snyder, R. G. *J. Phys. Chem.* **1991**, *95*, 938.
(9) Dorset, D. L. *Macromolecules* **1991**, *24*, 6521.
(10) Dorset, D. L. *Macromolecules* **1990**, *23*, 623.
(11) Dorset, D. L.; Hanlon, J.; Karet, G. *Macromolecules* **1989**, *22*, 2169.
(12) Wittmann, J. C.; Hodge, A. M.; Lotz, B. *J. Polym. Sci., Polym. Phys. Ed.* **1983**, *21*, 2495.
(13) Dorset, D. L. *Adv. Electronics Electron Phys.* **1994**, *88*, 111.
(14) Dorset, D. L. *Macromolecules* **1987**, *20*, 2782.
(15) Nyburg, S. C.; Potworowski, J. A. *Acta Crystallogr.* **1973**, *B29*, 347.
(16) Dorset, D. L. *Macromolecules* **1986**, *19*, 2965.
(17) Snyder, R. G.; Goh, M. C.; Srivatsavoy, V. J. P.; Strauss, H. L.; Dorset, D. L. *J. Phys. Chem.* **1992**, *96*, 10008.
(18) Mazee, W. M. *Prepr.–Am. Chem. Soc., Div. Petr. Chem.* **1958**, *3* (4), 35.
(19) Matheson, R. R., Jr.; Smith, P. *Polymer* **1985**, *26*, 288.
(20) Broadhurst, M. G. *J. Res. Natl. Bur. Stand.* **1962**, *66A*, 241.
(21) Snyder, R. G.; Conti, G.; Strauss, H. L.; Dorset, D. L. *J. Phys. Chem.* **1993**, *97*, 7342.
(22) Clavell-Grunbaum, D.; Strauss, H. L.; Snyder, R. G., to be published.
(23) Dorset, D. L. *Acta Crystallogr.*, in press.
(24) Dorset, D. L.; Annis, B. K. *Macromolecules*, submitted.

MA950844G